Mesoscopic two-phase model for describing apparent slip in micro-channel flows

2006 Europhys. Lett. 74 651

(http://iopscience.iop.org/0295-5075/74/4/651)

EUROPHYSICS LETTERS 15 May 2006

Europhys. Lett., **74** (4), pp. 651–657 (2006)
DOI: 10.1209/epl/i2006-10022-0

Mesoscopic two-phase model for describing apparent slip in micro-channel flows

R. Benzi[1], L. Biferale[1], M. Sbragaglia[1], S. Succi[2] and F. Toschi[2,3]

[1] *Dipartimento Fisica & INFN, Università Tor Vergata - via della Ricerca Scientifica 1 00133, Roma, Italy*
[2] *CNR-IAC - Viale del Policlinico 137, 00161 Roma, Italy*
[3] *INFN - via Saragat 1, 44100 Ferrara, Italy*

received 16 January 2006; accepted in final form 22 March 2006
published online 12 April 2006

PACS. 47.55.D- – Drops and bubbles.
PACS. 83.50.Rp – Wall slip and apparent slip.
PACS. 47.11.-j – Computational methods in fluid dynamics.

Abstract. – The phenomenon of apparent slip in micro-channel flows is analyzed by means of a two-phase mesoscopic lattice Boltzmann model including non-ideal fluid-fluid and fluid-wall interactions. The weakly inhomogeneous limit of this model is solved analytically. The present mesoscopic approach permits to access much larger scales than molecular dynamics, and comparable with those attained by continuum methods. However, at variance with the continuum approach, the existence of a gas layer near the wall does not need to be postulated *a priori*, but emerges naturally from the underlying non-ideal mesoscopic dynamics. It is therefore argued that a mesoscopic lattice Boltzmann approach with non-ideal fluid-fluid and fluid-wall interactions might achieve an optimal compromise between physical realism and computational efficiency for the study of channel micro-flows.

The microscopic physics underlying fluid/solid interactions is fairly rich and complex, for it depends on specific details of molecular interactions as well as on the micro-geometrical details of the boundary. However, on a macroscopic scale, these details can often be safely ignored by assuming that the net effect of surface interactions is simply to prevent any relative motion between the solid walls and the fluid elements next to them. This is the so-called "no-slip" boundary condition, which forms the basis of mathematical treatments of bounded flows as continuum media [1]. No-slip boundary conditions are extremely successful in describing a huge class of viscous flows. Yet, the evidence is that certain classes of viscous flows *do* slip on the wall. Recent advances in microfluidics experiments [2], as well as numerical investigations [3–7], have identified the conditions which seem to underlie the validity of the no-slip assumption. Namely: i) single-phase flow; ii) wetted surfaces and iii) low levels of shear rates. Under such conditions, careful experiments have shown that fluid comes to rest within a few molecular diameters from the surface [8–11]. Conditions i)-iii) are not exhaustive, though. For instance, partial slips of simple (Newtonian) flows, such as alkanes and water, is predicted by an increasing number of experiments [12–15] and simulations [3–7] (see [16] for a review on experiments and numerics). Under this state of affairs, there appears to be a great need

to provide a convincing, and possibly general, theoretical picture for the onset of slip motion. Among others, an increasingly popular explanation is that the flowing fluid would develop a lighter (less dense) phase and dynamically segregate it in the form of a thin film sticking to the wall [17,18]. This thin film would then provide a "gliding" surface for the bulk fluid which would slip on it without ever coming in contact with the solid wall. This gives rise to the so-called *apparent slip* phenomenon, that is, the extrapolated bulk flow speed would vanish far-out away from the wall, even though the actual flow speed in the film does vanish exactly at the wall location. This film-picture is very appealing, but still in great need of theoretical clarification. In particular, the underlying mechanisms of film formation are still under question: are they generic or detail-driven? In this paper, we shall propose that film formation is a generic phenomenon, which can be captured by a one-parameter mesoscopic approach, lying in between the microscopic (atomistic) and macroscopic (continuum) levels. The mesoscopic approach is based on a minimal two-phase (lattice) Boltzmann equation (LBE) [19–21], including non-ideal interactions [22–25], which can drive dynamic phase transitions. At variance with previous attempts using single-phase LBE with a mixture of free-slip and bounce-back boundary conditions to mimic different slippage properties at the boundaries [26] here we aim at investigating in deeper detail the origin of a finite slip lenght by resolving the density variations in the proximity of the walls. The only free parameter in the two-phase LBE here adopted is the strength of these non-ideal (potential energy) interactions. Hopefully, the present mesoscopic approach provides an optimal compromise between the need of including complex physics (phase transition) not easily captured by a continuum approach, and the need of accessing experimentally relevant space-time scales which are out of reach to microscopic Molecular Dynamics (MD) simulations [3,5–7]. In particular, at variance with the macroscopic approach, the gas film does not need to be postulated *a priori*, but emerges dynamically from the underlying mesoscopic description, by progressive switching of potential interactions. One major advantage of this formulation is that it allows to develop a simple and straightforward analytical interpretation of the results, based on the macroscopic limit of the model achieved by a standard Chapman-Enskog expansion, as well as of the effective slip length arising in the flow. The lattice Boltzmann model, used in this paper to describe multiple phases, has been developed by Shan and Chen in [22] (hereafter SC), well documented in the literature. Among the basic facts to recall, the model is a minimal discrete version of the Boltzmann equation, and reads as follows:

$$f_l(\boldsymbol{x}+\boldsymbol{c}_l,t+1)-f_l(\boldsymbol{x},t)=-\frac{1}{\tau}\left(f_l(\boldsymbol{x},t)-f_l^{(eq)}(\boldsymbol{x},t)\right)+F_l, \tag{1}$$

where $f_l(\boldsymbol{x},t)$ is the probability density function associated to a mesoscopic velocity $\boldsymbol{c}_l$, τ is a mean collision time, $f_l^{(eq)}(\boldsymbol{x},t)$ the equilibrium distribution that corresponds to the Maxwellian distribution in the fully continuum limit and, finally, F_l is an external forcing to be defined later. The bulk interparticle interaction is proportional to a free parameter, $\mathcal{G}_b$, entering the balance equation for the momentum change:

$$\frac{\mathrm{d}(\rho\boldsymbol{u})}{\mathrm{d}t}=\mathcal{G}_b\sum_l w_l\Psi\left[\rho(\boldsymbol{x})\right]\Psi\left[\rho(\boldsymbol{x}+\boldsymbol{c}_l)\right]\boldsymbol{c}_l, \tag{2}$$

being w_l the equilibrium weights and Ψ the potential function which describes the fluid-fluid interaction triggered by density variation. By Taylor-expanding eq. (2) one recovers, in the hydrodynamical limit, the equation of motion for a non-ideal fluid with equation of state $P=c_s^2(\rho-\frac{1}{2}\mathcal{G}_b\Psi^2(\rho))$, c_s being the sound speed velocity. With the choice $\Psi(\rho)=1-\exp[-\rho/\rho_0]$ with $\rho_0=1$ a reference density, the model supports phase transitions whenever the control parameter exceeds the critical threshold $\mathcal{G}_b>\mathcal{G}_b^c$. In our case, $\mathcal{G}_b^c=4$ for an averaged density $\langle\rho\rangle=\log(2)$.

We consider $\mathcal{G}_b$ as an external control parameter, with no need of responding to a self-consistent temperature dynamics. It has been pointed out [27] that the SC model is affected by spurious currents near the interface due to lack of conservation of local momentum. This criticism can be ruled out once the *instantaneous* pre- and post-collisional currents are replaced by a time average over a collisional time [28]. Let us now consider the main result of this letter, namely the critical interplay between the bulk physics and the presence of wall effects. In fact, in order to make contact with experiments and MD simulations, it is important to include fluid-wall interactions, and notably a parametric form of mesoscopic interactions capable of mimicking wettability properties as described by contact angles between droplets and the solid wall [29]. This effect is achieved by assuming that the interaction with the wall is represented as an external force F_w normal to the wall and decaying exponentially [25,30], *i.e.*

$$F_w(\boldsymbol{x}) = \mathcal{G}_w \rho(\boldsymbol{x}) e^{-|\boldsymbol{x}-\boldsymbol{x}_w|/\xi}, \tag{3}$$

where $\boldsymbol{x}_w$ is a vector running along the wall location and ξ the typical length-scale of the fluid-wall interaction, also known as the Kac range parameter [30].

Equation (3) has been recently used in a similar study to investigate the formation of a depletion layer close to the wall [31]. Previously, by using a slightly different LBE scheme, it has been used to show how the wetting angle depends on the ratio $\mathcal{G}_w/\mathcal{G}_b$ in the presence of phase coexistence between vapor and liquid [25]. Here we want to study the opposite situation, *i.e.* the effects of $\mathcal{G}_w$ when the thermodynamically stable bulk physics is governed by a single phase. The main result is that the presence of the wall may trigger a local phase coexistence inducing the formation of a less dense phase in the vicinity of the walls and an *apparent* slip of the bulk fluid velocity profile extrapolated at the wall location.

In the single-phase situation one cannot use the natural matching with the vapour-liquid interface in order to extract the physical units of the grid spacing. The only way to match the physical dimensions is via the pressure definition $P = P_{lu} k_b T/(\Delta x)^3$, where P_{lu} is the pressure in lattice units, k_b the Boltzmann constant and Δx the lattice spacing. Doing this, we obtain $\Delta x \sim 1\,\mathrm{nm}$ at room temperature and atmospheric pressure.

Equations (1)-(3) have been numerically solved for different values of the parameters $\mathcal{G}_b, \mathcal{G}_w$ and ξ in a two-dimensional channel with periodic boundary conditions in the stream-wise x direction, being $y = 0$ and $y = L_y$ the wall positions ($L_y = 80\Delta x$ for the present calculation). The sign of $\mathcal{G}_w$ is such to give a repulsive force for the liquid particles at the wall. The flow is driven by a constant pressure gradient in the x direction $F_i = \delta_{i,x}\partial_x P_0$. No-slip boundary conditions (*i.e.* bounce back boundary conditions with no constraint on the density) are used at the wall. These boundary conditions are consistent with the fact that the Knudsen number of the flow is well below unity. For small Knudsen numbers, *i.e.* in the large-scale limit, the numerical solutions have been checked against its weakly inhomogeneous macroscopic hydrodynamic limit, namely

$$\begin{aligned} &\partial_t \rho + \partial_i(u_i\rho) = 0, \qquad P = c_s^2\rho - V_{eff}(\rho), \\ &\rho\left[\partial_t u_i + (u_j\partial_j)u_i\right] = -\partial_i P + \nu\partial_j(\rho\partial_i u_j + \rho\partial_j u_i) + F_i, \end{aligned} \tag{4}$$

where subscripts i, j run over the two spatial dimensions, $\nu = c_s^2(\tau - 1/2)$ and P is the total pressure consisting of an ideal-gas contribution, $c_s^2\rho$, plus the so-called excess pressure, V_{eff}, due to potential-energy interactions. The expression of V_{eff} in terms of both $\mathcal{G}_b$ and $\mathcal{G}_w$ reads: $V_{eff}(\rho) = \frac{c_s^2}{2}\mathcal{G}_b(1 - \exp[-\rho])^2 + \mathcal{G}_w \int_0^y \mathrm{d}s\rho(s)\exp[-s/\xi]$. Let us notice that the continuum equation (4) naturally predicts the increase of the mass flow rate in the presence of a density profile which becomes more and more rarefied by approaching the wall [17]. Indeed,

under stationary conditions, the continuity equation in (4) reduces to $\partial_y(\rho u_y) = 0$, which, because of the boundary conditions, implies $\rho u_y = 0$, *i.e.* $u_y = 0$ everywhere. Thus, in a homogeneous channel along the stream-wise direction, the velocity u_x satisfies the equation

$$\nu\partial_y(\rho\partial_y u_x) = -\partial_x P_0. \tag{5}$$

In the new variable, $y' = y - H$, where $H = L_y/2$, we may express the solution of (5) as

$$u_x(y') = -\int_{y'}^{H} \frac{s\partial_x P_0}{\nu\rho(s)}\mathrm{d}s. \tag{6}$$

Using (6) and assuming that density variations are concentrated in a smaller layer of thickness δ near the wall, we can estimate the mass flow rate Q_{eff} for small δ as

$$\frac{Q_{eff}}{Q_{pois}} = 1 + \frac{3}{2}\frac{\Delta\rho_w}{\rho_w}\frac{\delta}{H}, \tag{7}$$

where Q_{pois} corresponds to the Poiseuille rate $2\partial_x P_0 H^3/3\nu$ valid for incompressible flows with no-slip boundary conditions. In eq. (7), the quantity $\Delta\rho_w$ is defined as the difference between ρ computed in the center of the channel and ρ_w computed at the wall. The effective slip length is then usually defined in terms of the increment in the mass flow rate [16]:

$$\lambda_s \sim \delta\Delta\rho_w/\rho_w. \tag{8}$$

This is the best one can obtain by using a purely continuum approach. Our eq. (7) exhibits the same dependence on the inverse wall density as eq. (16) of [32]. However, the prefactor in eq. (16) of [32] takes into account atomistic details which in our case are represented by the single parameter, G_w. The added value of the mesoscopic approach here proposed consists in the possibility to directly compute the density profile, and its dependency on the underlying wall-fluid and fluid-fluid physics. To this purpose, we consider the momentum balance equation in (4) for the direction normal to the wall, $i = y$. Since $u_y = 0$, we simply obtain $\partial_y P = 0$, *i.e.*

$$c_s^2\partial_y\rho - 2\mathcal{G}_b c_s^2(1 - e^{-\rho})e^{-\rho}\partial_y\rho - \mathcal{G}_w\rho e^{-y/\xi} = 0. \tag{9}$$

Let us first study the effects of the wall in (9) by setting $\mathcal{G}_b = 0$. One can easily obtain $\log(\rho(y)/\rho_w) = \frac{\xi\mathcal{G}_w}{c_s^2}(1-\exp[-y/\xi])$, which enables us to estimate $\Delta\rho_w = \rho_w(\exp[\xi\mathcal{G}_w/c_s^2]-1)$. Using (8), we obtain for the effective slip-length:

$$\lambda_s/\xi \sim e^{\xi\mathcal{G}_w/c_s^2} \qquad\qquad [\mathcal{G}_b = 0]. \tag{10}$$

As expected, eq. (10) provides the dimensionless slip length in units of the interatomic length, as a function of the dimensionless ratio of potential to thermal energy [33]. We now turn our attention to the non-trivial interference between bulk and wall physics whenever $\mathcal{G}_b > 0$. Defining the bulk pressure as $P_b = c_s^2\rho - \frac{c_s^2}{2}\mathcal{G}_b(1-\exp[-\rho])^2$, we can rewrite eq. (9) to highlight its physical content as follows:

$$\log\left(\frac{\rho(y)}{\rho_w}\right) = \xi\mathcal{G}_w(1 - e^{-y/\xi})/\overline{\partial P_b/\partial\rho}, \tag{11}$$

where the bulk effects appear only through the following term:

$$\overline{\frac{\partial P_b}{\partial\rho}} \equiv \frac{1}{\log(\rho(y)/\rho_w)}\int_{\rho(0)}^{\rho(y)}\frac{\partial P_b}{\partial\rho}\frac{\mathrm{d}\rho}{\rho}. \tag{12}$$

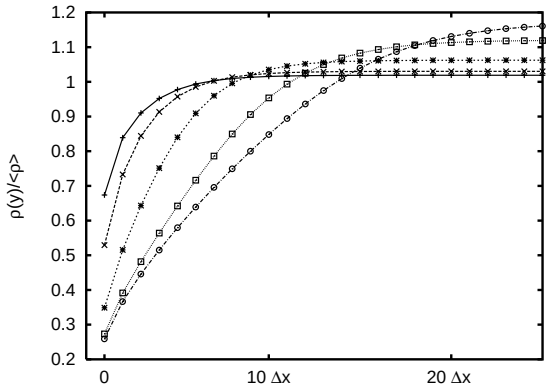

Fig. 1 – Rarefaction effects in the full-interaction case $\mathcal{G}_w,\ \mathcal{G}_b \neq 0$. Density profiles normalized to the average density are plotted as a function of the distance from the wall (y). The wall interactions have been fixed assuming $\mathcal{G}_w = 0.03$ and $\xi = 2\Delta x$. The following values of $\mathcal{G}_b$ are considered: $\mathcal{G}_b = 1.5$ (+), $\mathcal{G}_b = 2.5$ (×), $\mathcal{G}_b = 3.5$ (∗), $\mathcal{G}_b = 3.9$ (□), $\mathcal{G}_b = 3.98$ (○). We remind that the bulk phase transition is set at $\mathcal{G}_w^c = 4$. Here, the lattice spacing $\Delta x \sim 1\,\mathrm{nm}$ as explained in the text. As a result, we observe that δ, the rarefaction layer thickness, is ranging between 4 nm and 20 nm [34] .

Equation (11) highlights two results. First, the effect of the bulk can always be interpreted as a renormalization of the wall-fluid interaction by $\mathcal{G}_w^R \equiv \mathcal{G}_w/\overline{\partial P_b/\partial\rho}$. Second, as is evident from the above expression, one must notice that near the bulk critical point where $\partial P_b/\partial\rho \to 0$, the renormalizing effect can become unusually great. In other words, the presence of the wall may locally push the system toward a phase transition even if the bulk physics is far from the transition point. As a result, the effective slip length in the presence of both wall and bulk non-ideal interactions can be estimated as $\lambda_s \sim \xi \exp[\xi\mathcal{G}_w^R]$. In fig. 1 we show $\rho(y)$ for different values of $\mathcal{G}_b$ and $\mathcal{G}_w = 0.03$, $\xi = 2\Delta x$ as obtained by numerically integrating eqs. (1)-(3). The numerical simulations have been carried out by keeping fixed the value of $\langle\rho\rangle = \frac{1}{L_y}\int_0^{L_y}\rho(s)\mathrm{d}s = \log(2)$. As one can see, while $\mathcal{G}_b \to \mathcal{G}_c = 4$, the density difference $\Delta\rho_w$ between the center of the channel and the wall increases, as predicted by eq. (9). Consequently, the mass flow rate increases as shown in fig. 2. Let us notice in the same figure that also with $\mathcal{G}_w = 0$, the wall initiates a small rarefaction effect due to the fact that fluid particles close to the boundary are attracted only by particles in the bulk of the channel. What we showed here is that the combined actions of $\mathcal{G}_w$ and $\mathcal{G}_b \to \mathcal{G}_b^c$ may strongly increase the formation of this less dense region in the proximity of the surface. For a quantitative check, we have numerically integrated eqs. (9) and (6) for a given value $\langle\rho\rangle = \log(2)$. The analytical estimate for ρu_x is compared with the numerical results in fig. 3. This is a stringent test for our analytical interpretation. The result is that the analytical estimate is able to capture the deviations from a pure parabolic profile at approaching the wall region, where rarefaction effects are present. The crucial point in our analysis is that, even for very small $\mathcal{G}_w$, large apparent slip can occur in the channel if $\mathcal{G}_b$ is close to its critical value, *i.e.* the limit $\mathcal{G}_w \to 0$ and $\mathcal{G}_b \to \mathcal{G}_b^c$ do not commute. For example, let us consider the case when $\mathcal{G}_w \sim \epsilon \ll 1$, $\xi \sim \epsilon$ and $\mathcal{G}_b \sim \mathcal{G}_b^c - \epsilon^3$; we obtain $\overline{\frac{\partial P_b}{\partial\rho}} \sim \epsilon^3$ and therefore, $\lambda_s \sim \xi\exp[\xi\mathcal{G}_w^R] \sim \mathrm{O}(1)$ for $\epsilon \to 0$. The wall effect, parametrized by $\mathcal{G}_w$ and ξ, can act as a catalyzer in producing large apparent slip. Let us remark that in the limit of large channel ($H/\xi \to \infty$) and finite specific heat (*i.e.* $\overline{\partial P_b/\partial\rho} > 0$) the whole effect disappears and the standard Poiseuille flow profile is recovered.

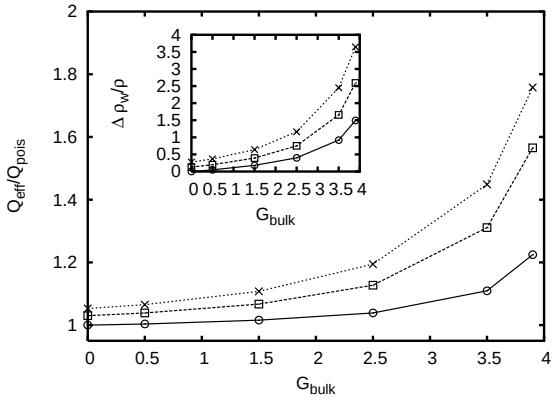

Fig. 2 – Increase of the mass flow rate with the coupling strength $\mathcal{G}_b$ of fluid-fluid bulk interactions. Fixing the wall correlation function $\xi = 2\Delta x$, we plot the mass flow rate (Q_{eff}) normalized to its Poiseuille value (Q_{pois}) as a function of $\mathcal{G}_b$ for different values of $\mathcal{G}_{wall}$: $\mathcal{G}_{wall} = 0.0$ ($\circ$), $\mathcal{G}_{wall} = 0.04$ ($\square$), $\mathcal{G}_{wall} = 0.08$ ($\times$). Inset: same as the main figure for $\Delta\rho_w/\rho$.

Most of the results shown in figs. 1 and 2 are conducive to the same physical picture emerging by MD numerical simulations [3, 4, 6, 7]. Our analysis points out that, close to the wall, one can observe a "local phase transition" triggered by the presence of the wall itself. In summary, we have shown that a suitable form of the lattice Boltzmann equation can be proposed in order to simulate apparent slip in microchannels. Slip boundary conditions arise spontaneously because, close to the wall, a "gas" layer is formed. If the system is close to a state where coexistence of different phases (liquid and gas) are thermodynamically achievable, then macroscopic slip effects can result. We have shown that for large-scale separation, the model reduces to a continuum set of hydrodynamical equations which explain the qualitative and quantitative behavior of the mass flow rate in terms of the model parameters, *i.e.* $\mathcal{G}_b$ and $\mathcal{G}_w$.

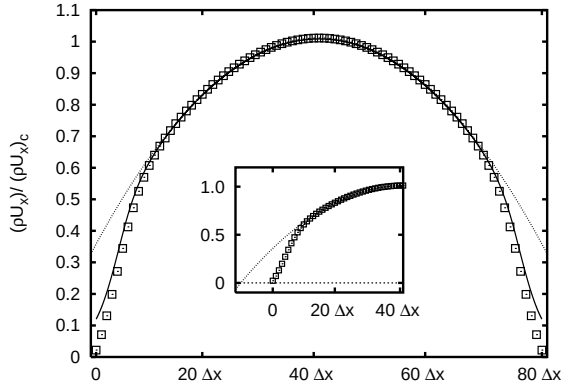

Fig. 3 – Momentum profile as a function of the channel height. We plot the momentum profile (ρu_x) normalized to its center channel value ($(\rho u_x)_c$) as a function of the distance from the wall (y). The results of numerical simulations ($\square$) with $\mathcal{G}_b = 3.5$, $\mathcal{G}_w = 0.08$ and $\xi = 2\Delta x$ are compared with the analytical estimate (continuous line) obtained solving eqs. (9) and (6). To highlight the rarefaction effect, the parabolic fit in the center channel region (dotted line) is plotted. Inset: estimate of the apparent slip length in the channel with the same parabolic fit as in the main figure.

* * *

We kindly thank S. Troian and J.-L. Barrat for useful comments and critical reading of the manuscript.

REFERENCES

[1] Massey B., *Mechanics of Fluids* (Chapman & Hall) 1989.
[2] Ho C.-M. and Tai Y.-C., *Annu. Rev. Fluid Mech.*, **30** (1998) 579; Tabeling P., *Introduction à la microfluidique* (Belin) 2003.
[3] Barrat J.-L. and Bocquet L., *Phys. Rev. Lett.*, **82** (1999) 4671.
[4] Cieplak M., Koplik J. and Banavar J. R., *Phys. Rev. Lett.*, **86** (2001) 803.
[5] Thompson P. and Troian S. M., *Nature*, **389** (1997) 360.
[6] Darhuber A. A. and Troian S. M., *Annu. Rev. Fluid Mech.*, **37** (2005) 425.
[7] Cottin-Bizonne C. *et al.*, *Eur. Phys. J. E*, **15** (2004) 427.
[8] Chan D. Y. C. and Horn R. G., *J. Chem. Phys.*, **83** (1985) 5311.
[9] Israelachvili J. N., McGuiggan P. M. and Homola A. M., *Science*, **240** (1988) 189.
[10] Klein J. and Kumacheva E., *Science*, **269** (1995) 816.
[11] Raviv U., Laurat P. and Klein J., *Nature*, **413** (2001) 51.
[12] Choi C., Johan K., Westin A. and Breuer K., *Phys. Fluids*, **15** (2003) 2897.
[13] Cheng J.-T. and Giordano N., *Phys. Rev. E*, **65** (2002) 031206.
[14] Pit R., Hervet H. and Leger L., *Phys. Rev. Lett.*, **85** (2000) 980.
[15] Joseph P. and Tabeling P., *Phys. Rev. E*, **71** (2005) 035303(R).
[16] Lauga E., Brenner M. P. and Stone H. A., *The no-slip boundary condition: a review*, cond-mat/0501557.
[17] Tretheway D. and Meinhart C., *Phys. Fluids*, **16** (2004) 1509.
[18] de Gennes P. G., *Langmuir*, **18** (2002) 3413.
[19] Higuera F. and Jimenez J., *Europhys. Lett.*, **9** (1988) 661; Higuera F., Succi S. and Benzi R., *Europhys. Lett.*, **9** (1989) 345.
[20] Benzi R., Succi S. and Vergassola M., *Phys. Rep.*, **222** (1992) 145.
[21] Karlin I., Ferrante H. and Oettinger C., *Europhys. Lett.*, **47** (1999) 182.
[22] Shan X. and Chen H., *Phys. Rev. E*, **47** (1993) 1815; **49** (1994) 2941.
[23] Swift M. R., Osborn W. R. and Yeomans J. M., *Phys. Rev. Lett.*, **75** (1995) 830.
[24] Verberg R., Pooley C. M., Yeomans J. M. and Balazs A. C., *Phys. Rev. Lett.*, **93** (2003) 1845011.
[25] Zhang J. and Kwok D., *Phys. Rev. E*, **70** (2004) 056701; Zhang J., Ling B. and Kwok D., *Phys. Rev. E*, **69** (2004) 032602.
[26] Benzi R., Biferale L., Sbragaglia M., Succi S. and Toschi F., *J. Fluid Mech.*, **548** (2006) 257.
[27] Nourgaliev R. R., Dinh T. N., Theofanous T. G. and Joseph D., *Int. J. Multiphase Flow*, **29** (2003) 117.
[28] Buick J. M. and Greated C. A., *Phys. Rev. E*, **61** (2000) 5307.
[29] de Gennes P. G., *Rev. Mod. Phys.*, **3** (1985) 827.
[30] Sullivan D. E., *J. Chem. Phys.*, **74** (1981) 2604.
[31] Harting J., Kunert C. and Herrmann H. J., *Lattice Boltzmann simulations of apparent slip in hydrophobic microchannels*, physics/0507026.
[32] Barrat J.-L. and Bocquet L., *Faraday Discuss.*, **112** (1999) 119.
[33] Blake T. D., *Colloids Surf.*, **47** (1990) 135.
[34] Doshi D. A., Watkins E. B., Israelachvili J. N. and Majewski J., *Proc. Natl. Acad. Sci. U.S.A.*, **102** (2005) 9458.